Characterization of Small Surface-Breaking Defects with Eddy Current Sensor Measurements

Stéphanie DUBOST, Laurence CHATELLIER, Fabien PEISEY, Eléctricité de France (EDF) Research and Development, France
Yves GOUSSARD, Raphaël GUICHARD, Biomedical Engineering Institute, Ecole Polytechnique de Montréal, Canada

Abstract. Usual NDE techniques do not easily produce satisfying estimates of the depth of a surface-breaking defect when this depth is below 5 mm. We propose to explore the capabilities of an advanced reconstruction method to characterize such surface-breaking defects from eddy current sensor measurements performed on mock-ups.
The proposed method is based on the regularization of inverse problems: when the information content of the measurements is poor, regularization techniques introduce *prior* information on the sought-for solution (the defect is made of air, for example) in order to improve the estimation results. The method is made up of two steps, which both make use of regularization. In the first step, the estimation of the characteristics of the inspected medium is performed while in the second step, the characteristics of the defect are estimated.
In this paper, we present how these regularization techniques are successfully applied to the characterization of surface-breaking defects in mock-ups, such as notches or cracks.

Introduction

Key power plant components must meet regulatory requirements throughout their lifetime. Should a critical defect be detected on a component, it has to be proven whether its dimensions are compatible with the acceptance criteria resulting from the mechanical requirements, and, if not, whether the component should be repaired or replaced. Thus, the ability to position and size measure defects in those major components is a key issue for the life management of plants, from both technical and economical standpoints.
Usual NDE techniques do not easily produce estimates of the depth of a surface-breaking defect when this depth is below 5 mm. This shallow values are generally considered as edging the ultrasonic techniques capabilities. On the other hand, eddy current techniques are sensitive in this area, but not adaptable to characterization in a straight-forward way. Such a classification of small depth defects may however be important in order to determine the best action to be undertaken in terms of replacement or repair.
In this paper we propose an approach based on eddy current measurement processing, by considering the problem as a so called *inverse problem*. Provided that a defect is present, the aim is to reconstruct a map of material relative conductivity which afterwards enables the operator to estimate several characteristics of the defect, among which its depth. This method has been previously proposed in [1], and is composed of two steps (medium characteristics estimation and defect estimation). In this paper, we present some

modifications of the defect estimation step which lead to improvements in the reconstruction results. We also present results on a mock-up defect that corresponds to a more realistic case.

1. Problem Statement

We consider an austenitic steel object to be inspected with the help of eddy current (EC) sensors. It is assumed that a surface-breaking defect is present, that it is isolated from other ones and that its shape is roughly that of a notch or a crack.
An EC sensor is moved on the surface of the component area containing the defect, along lines perpendicular to the direction of the defect length. If no defect is present, the electric field measured by the EC sensor is constant, whereas presence of a defect produces a variation of the electric field. Our goal is to use the set of EC measurements $\boldsymbol{y}$ to estimate the distribution of relative conductivity $\boldsymbol{x}$ in the area of interest. The relative conductivity is defined as the ratio $(\sigma_0-\sigma)/\sigma_0$, where σ_0 and σ respectively denote the austenitic steel and defect conductivities. The latter being generally equal to zero, the relative conductivity can be assumed to be either 0 (no defect) or 1 (presence of a defect).

2. Method

2.1 Modeling assumptions

We adopt the three-dimensional (3D), discretized framework schematically depicted in Figure 1.

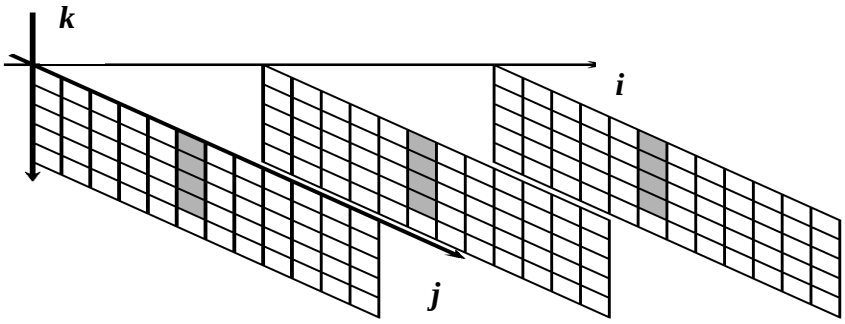

Figure 1 *Geometry of the discretized 3D problem. The probe collects measurements close to the surface k = 0 of the unknown medium.*

The probe collects measurements close to the surface $k = 0$ of the unknown medium. Our approach is based on a linearized form of the relationship between relative conductivity values $\boldsymbol{x}$ and measurements $\boldsymbol{y}$ whose expression is derived using minimal assumptions. More precisely, the linearity of the phenomena implies that the measurements $\boldsymbol{y}$ can be expressed as the sum of the contributions $\boldsymbol{y}_k$; $1 \leq k \leq K$ of each layer (constant value of index k) of the unknown medium. K denotes the total number of layers. In addition, the medium is assumed to be infinite in the i and j directions; consequently, the phenomena within each layer are shift-invariant and can therefore be expressed as a two-dimensional (2D) convolution product. Using a matrix notation, we can write:

$$\boldsymbol{y}_k = \boldsymbol{H}_k \boldsymbol{x}_k = \boldsymbol{X}_k \boldsymbol{h}_k \quad (1)$$

where the components of the 2D point spread function (PSF) which characterizes layer k and the relative conductivity components of layer k are concatenated in vectors $\boldsymbol{h}_k$ and $\boldsymbol{x}_k$,

respectively. Matrices $\boldsymbol{H}_k$ and $\boldsymbol{X}_k$ are built from the elements of $\boldsymbol{h}_k$ and $\boldsymbol{x}_k$ in order to implement a 2D convolution product. From the above equations, we obtain:

$$\boldsymbol{y} = \sum_{k=1}^{K} \boldsymbol{y}_k = \boldsymbol{H}\boldsymbol{x} + \boldsymbol{n} = \boldsymbol{X}\boldsymbol{h} + \boldsymbol{n} \tag{2}$$

where matrices $\boldsymbol{H}$ and $\boldsymbol{X}$ and vectors $\boldsymbol{x}$ and $\boldsymbol{h}$ are built by appropriate concatenation of quantities $\boldsymbol{H}_k$, $\boldsymbol{X}_k$, $\boldsymbol{x}_k$ and $\boldsymbol{h}_k$; $1 \leq k \leq K$, respectively and where $\boldsymbol{n}$ denotes a noise vector that represents all phenomena not accounted for by the model.

2.2 Approach

In the proposed approach, two stages are required: (*i*) utilization of actual data collected on known defects for estimating the set of PSFs which characterizes the probe/medium response; (*ii*) estimation of unknown defects using the PSFs obtained at the first stage. At both stages, the estimation problem may be ill-conditioned in the sense that the information content and relative size of measured data is rather limited, with the consequence of a high sensitivity of the solutions to observation noise $\boldsymbol{n}$ [2]. In order to cope with this situation, some form of regularization must be used. Here regularization is achieved by using a *penalized least-squares estimator* at each stage. The penalty term is selected so as to produce an acceptable trade-off between some desirable properties of the estimates and the numerical efficiency of the resulting optimization procedure. These points are detailed in the next two sections.

2.3 PSF Estimation

Due to the nature of the underlying physical phenomena, we assume that each PSF of the set is smooth and that the shapes of the PSFs vary slowly with the depth index *k*. These characteristics can be encouraged by a quadratic penalty term on, e.g., the gradient of the estimate along the three axis directions. The corresponding penalized least-squares criterion takes the following form:

$$J(\boldsymbol{h}; \boldsymbol{y}) = \left\| \boldsymbol{y} - \boldsymbol{X}\boldsymbol{h} \right\|^2 + \lambda \left\| \boldsymbol{D}\boldsymbol{h} \right\|^2 \tag{3}$$

where $\boldsymbol{D}$ represents the discrete gradient operator ($\boldsymbol{D}$ is actually the sum of the first difference operators along the three axis directions) and where λ is a weighting parameter referred to as the *regularization parameter*. In this step, $\boldsymbol{D}$ may also contain an additional operator proportional to identity. Note that the form $\boldsymbol{y} = \boldsymbol{X}\,\boldsymbol{h} + \boldsymbol{n}$ of the model is used at this stage as it is best suited to the estimation of vector $\boldsymbol{h}$. Note also that criterion $J(\boldsymbol{h};\boldsymbol{y})$ is quadratic with respect to $\boldsymbol{h}$ and that the solution can be expressed in a closed form. However evaluation of the closed form solution is impossible in practice due to the size of matrices $\boldsymbol{X}$ and $\boldsymbol{D}$. In order to circumvent the difficulty, we chose to minimize $J(\boldsymbol{h};\boldsymbol{y})$ iteratively using a Polak-Ribiere conjugate gradient algorithm [3]. The value of regularization parameter λ can be determined either heuristically or using estimation techniques such as generalized cross-validation [4], the chosen approach here being the heuristically one.

2.4 Reconstruction of the unknown medium

The approach to the estimation of $\boldsymbol{x}$ when the PSFs are known is essentially similar to the one described in the previous paragraph. However, the defects can hardly be considered smooth since they are made up of homogeneous regions separated by sharp discontinuities. In order to account for this characteristic, the penalty term considered is made of two components:

- the first one is based upon an *edge-preserving, convex potential function* φ applied to all differences between pairs of neighboring components of $\boldsymbol{x}$. Function $\varphi(u) = (\mu^2+u^2)^{1/2}$, where μ represents a scale factor (similar to the Huber function used in edge-preserving image reconstruction [5]) is used. If compared to the square function used in the PSF estimation step, this function applied to the discrete gradient of $\boldsymbol{x}$ ($\boldsymbol{Dx}$) allows greatest values of $\boldsymbol{Dx}$ to appear thanks to a least penalization of these values. Higher values of $\boldsymbol{Dx}$ corresponding to discontinuities of $\boldsymbol{x}$, this penalization is expected to help us recovering the defect.
- the second one is a term that takes into account the expected binary value of x (0 if there is no defect, 1 if there is one). The function ψ used is derived from φ and is defined as

$$\psi(u) = \tilde{\varphi}(u) + \tilde{\varphi}(u-\mathbf{1}) \quad \text{where} \quad \tilde{\varphi}(u) = \mu + \sqrt{\delta^2 + u^2} - \sqrt{\mu^2 + u^2}$$

  The modification in the method presented previously in [1] lies in this "binary" penalty term: the corresponding term used at this stage in [1] was $\varphi(0)$.

The different penalization function used are presented in Figure 2 below.

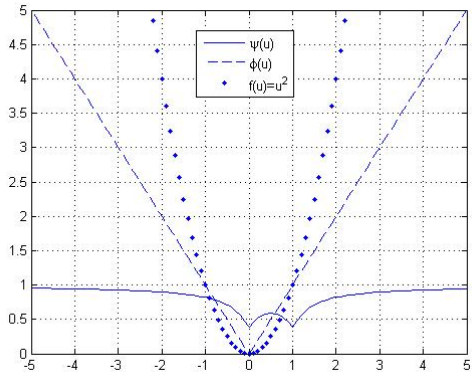

Figure 2 Shape of penalization functions $\varphi(u)$ *and* $\psi(u)$ used.

Therefore, the penalized least-squares criterion used for reconstructing unknown defects takes the following form:

$$J(\mathbf{x};\mathbf{y}) = \left\|\mathbf{y} - \mathbf{H}\mathbf{x}\right\|^2 + \lambda_0 \psi(\mathbf{x}) + \lambda_1 \varphi(\mathbf{D}\mathbf{x}) \qquad (4)$$

where, for any vector $\boldsymbol{v}$, the notation $\varphi(\boldsymbol{v})$ is used in place of $\Sigma\varphi(v_i)$, the summation being extended to all components of $\boldsymbol{v}$. λ_0 and λ_1 denote the regularization parameters and $\boldsymbol{D}$ represents the same gradient operator as in the previous paragraph. Note that at this stage, the form $\boldsymbol{y} = \boldsymbol{H}\,\boldsymbol{x} + \boldsymbol{n}$ of the model is used because it is best suited to the estimation of $\boldsymbol{x}$.

Criterion $J(\boldsymbol{x};\boldsymbol{y})$ does not remain convex because of the non convexity of function ψ(u), hence the existence of a unique minimum is not guaranteed anymore by the iterative descent algorithms used. Still, the same conjugate gradient technique has been used to minimize this criterion (4) because of its adequate trade-off between numerical efficiency, convergence speed and ease of implementation . Although the result is not guaranteed to be the global minimizer of criterion (4), the use of such a technique is justified by the fact that reconstruction results have been improved if compared with the previous convex version of

this criterion (which was expressed as $\varphi(\boldsymbol{x})$ instead of $\psi(\boldsymbol{x})$, see [1]). Finally, the regularization parameters were determined in a heuristic manner from the reconstruction of known test defects.

3. Results

3.1 Experimental data

Two probes were used in our experiments:

- the first one, named COM probe, is an air cored coil with a 3.5 mm external diameter used in impedance mode at frequency 300kHz.
- The second one, named SEP probe, is a transmit/receive probe with T/R distance 6 mm and coil outer diameter 2.8 mm, used at frequency 300 kHz.

For both of them, the acquisition step was equal to 0.2 mm along the two directions. The experimental data were obtained by inspection of austenitic stainless steel 304L mock-ups, which contain several EDM notches. The notches characteristics were: length (15 or 20 mm), width (0.1, 0.2 or 0.3 mm), depth (0.5, 1, 2, 3, 4, 5, 6 mm), and shape (rectangular or semi-elliptical). Another set of data was obtained by inspection of a different austenitic stainless steel mock-up containing a small surface-breaking defect (crack).
The discretization step of the medium was equal to 0.2 mm along directions *i* and *j*, and to 0.5 mm along direction *k*. The relative conductivity was estimated up to an 8 mm depth, which corresponds to 16 layers along direction *k*.

3.2 PSF estimation

3.2.1 Main settings

In a preliminary step, one must *select a data set* from which the PSFs will be estimated. At the PSF estimation stage, the rectangular notches with length 15 mm and width 0.2 mm were used. As the choice of a data set is not obvious, we studied the robustness of the estimation with respect to this choice. It appeared that the choice of a set of defects with depths ranging from a minimum to a maximum value to be reconstructed was more important than the actual number of defects being considered. Furthermore, the study indicated that the data set should be chosen so that each data provides additional information. The results presented in this paper are obtained with the PSF estimated with notches with depths {0.5, 1, 2, 3, 4, 5, 6} mm.
The *PSF size* has also to be set before performing the estimation. As there was no isolated point defect in the data set, the PSF size could not be assessed by direct observation of the measurements. Selection of the PSF size was performed by making sure that the PSF decreased correctly toward zero at their support boundaries and that the synthesized data from the estimated PSFs corresponding to different sizes, fit well with the real data. Here, the selected sizes here were 13.4 x 8.2 mm along the the *i* and *j* directions.
In our experiments, the value of *regularization parameter* λ that appears in (3) was set heuristically by observing the shape of the estimated PSFs: the larger this regularization parameter is, the "flatter" the estimated PSF is. At this step, the regularization parameters were set to small values, firstly because the ratio between the number of measurements and the number of parameters to estimate was large, and secondly because the quality of the measurements was good (high SNR).

3.2.2 PSF estimation results

Examples of PSF estimation results are shown in Figures 3 to 6, for the two probes used. For each probe (respectively COM and SEP):

- the first figure (figures 3 and 5 respectively) presents the modulus of the PSF for the first layer (corresponding to the [0 – 0.5] mm depth) on the left hand side, and the modulus for the first four layers (i.e. up to a 2 mm depth) on the right hand side;
- the second one (figures 4 and 6 respectively) shows on the left hand side the longitudinal cross-sections of real and synthesized measurements on notches with the following characteristics: 15mm long, 0.2 mm width and depth between 0.5 and 6 m. On the right hand side, modulus of real and synthesized 2mm depth defect are shown.

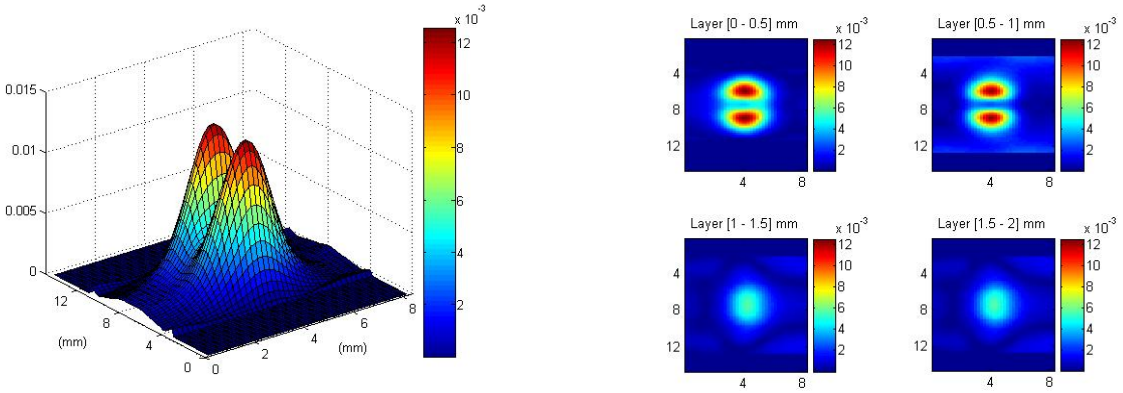

Figure 3 COM probe: PSF. Left hand side: 3D shape of the modulus of the PSF first layer, Right hand side: 2D modulus of the PSF frome fisrt ([0-0.5] mm) to fourth layer ([1.5-2] mm)

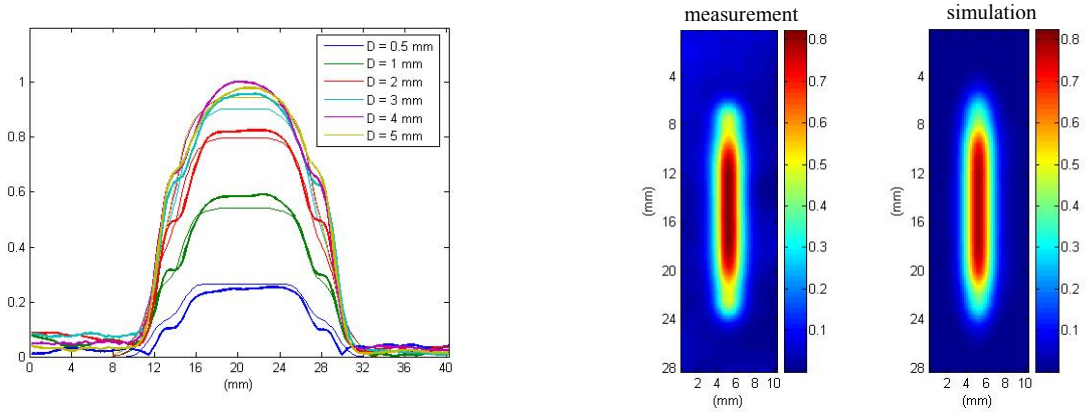

Figure 4 COM probe: Comparison between real and synthesized data. Left hand side: longitudinal cross-section of real (bold line) and synthesized data (normal line) along the 15 mm notches. Right hand side: modulus of the real data (left hand side) and the synthesized data (right hand side) for the 2mm depth, 15 mm long, 0.2 mm width notch

As can be seen in figures 3 and 5, the estimated PSF corresponding to the different probes have different shapes. The PSF of the COM probe has two humps on the first two layers, which seems to be realistic if we consider simulations of measurements on small defects (small depth and length defects, close to point defect), for which those humps also appear.

The SEP probe PSF has only one hump for each layer, which also seems to be realistic if compared to simulations.

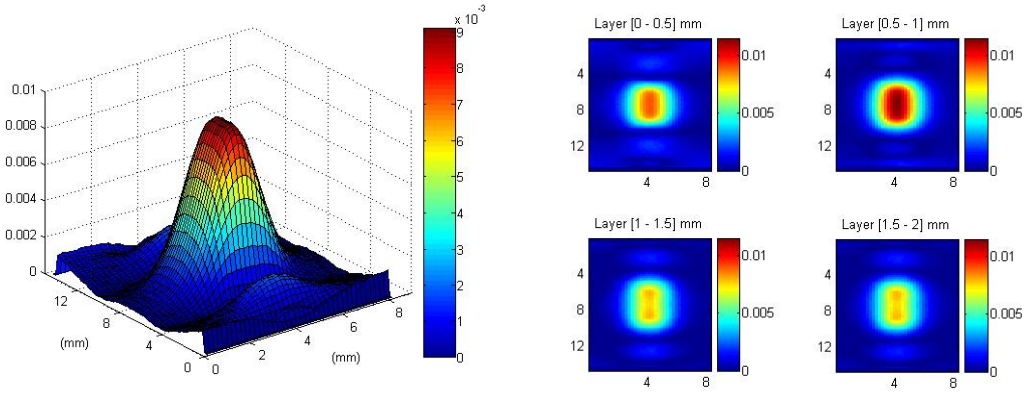

Figure 5 SEP probe: PSF. Left hand side: 3D shape of the modulus of the PSF first layer, Right hand side: 2D modulus of the PSF frome fisrt ([0-0.5] mm) to fourth layer ([1.5-2] mm)

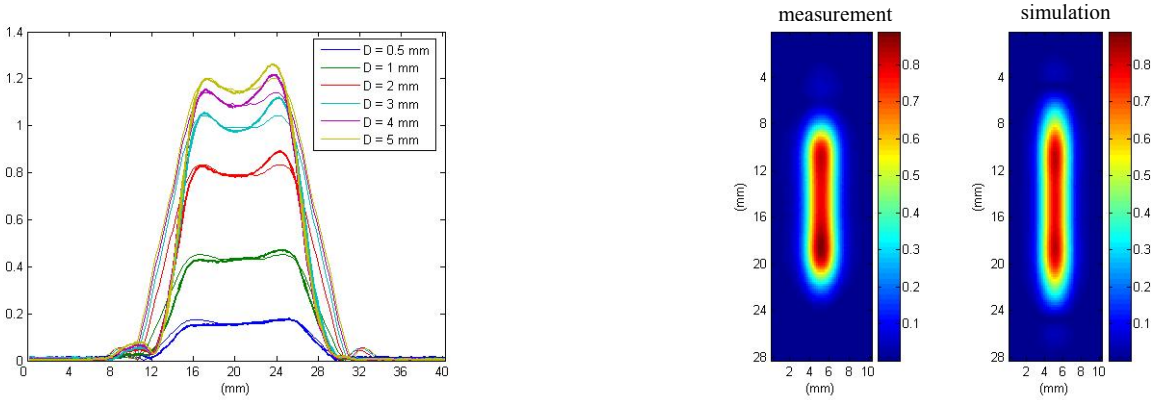

Figure 6 SEP probe: Comparison between real and synthesized data. Left hand side: longitudinal cross-section of real (bold line) and synthesized data (normal line) along the 15 mm notches. Right hand side: modulus of the real data (left hand side) and the synthesized data (right hand side) for the 2mm depth, 15 mm long, 0.2 mm width notch

In figures 4 and 6, the quality of the modeling assumptions leading to model (2) can be evaluated: the comparison between the simulated data (normal line) and the real data (bold line) corresponding to the same defects leads to the following conclusions: both of the PSF allow to simulate data quite close to the real ones. For the SEP probe, the simulations are better on the high amplitude area of the data, and worse close to the boundary of the defects. For COM probe, the simulations are not as good as the SEP ones in the high amplitude area, but the boundaries are better reproduced. Those simulations are close to the actual measurements , and therefore validate the simplified linear model (2).

3.2 Reconstruction of the unknown medium

3.2.1 Main settings

At this stage also, the regularization parameters that appear in (4) must be set before performing the reconstruction. Here too, we used a heuristic approach in which some

known defects (in our case: two) were reconstructed for different hyperparameter values. Using dichotomy techniques, we chose the parameters that gave the best results in terms of contrast (the reconstruction is as clean as possible) and precision (the estimated characteristics are as close to the real ones as possible). Then, those regularization parameters values were set and used for all other reconstructions.

3.2.2 Reconstruction results

Results on rectangular notches and on a crack (on mock-ups) are presented in Table 1 below. Following conclusions can be drawn:

- The *depth* is correctly estimated for rectangular notches up to 3 mm. For deeper defects, because of the low sensibility of the probe, the measurements are roughly the same. Hence, the associated reconstruction results underestimate the defect depth. For this reason, all reconstruction results with depth over 3 mm should all be considered only as "deeper than 3 mm" defects.
- The model (2) gives about the same simulation results for the two following defects: width l and depth D, or width $2l$ and depth $D/2$. This justifies the last two results obtained with the SEP probe set of data (see Table 1). This is due to the inadequation of the simplified model in the width direction. Constraining the width to be the same as the one of rectangular defects used in the PSF estimation stage leads to improved depth estimation.

Table 1 Characteristic estimations obtained from reconstruction results

Type of defect	Rectangular notches with length 15 mm							Crack
Real depth (mm)	0.5	1	2	3	4	5	6	4
Estimated depth corresponding to COM measurements	0.5	1	2	2.5	3	3	3.5	3
Estimated depth corresponding to SEP measurements	0.5	1	2	2.5	3	2.5*	2*	2.5

* The values with a star are underestimated due to an overestimation of the width: 0.4 mm instead of 0.2 mm.

Two reconstruction illustrations are shown in Figure 7 for the two probes COM (left hand side) and SEP (right hand side). The defect was the crack which depth is supposed to be around 4 mm. The results shown are plotted after a "binarisation" of the estimated relative conductivities (this consists in putting the estimation either to 0 or to 1 by comparison with a threshold value, close to 0.5). The result is quite good for both of the probes, as the estimated depths were 3 and 2.5 mm respectively for the COM and SEP probes.

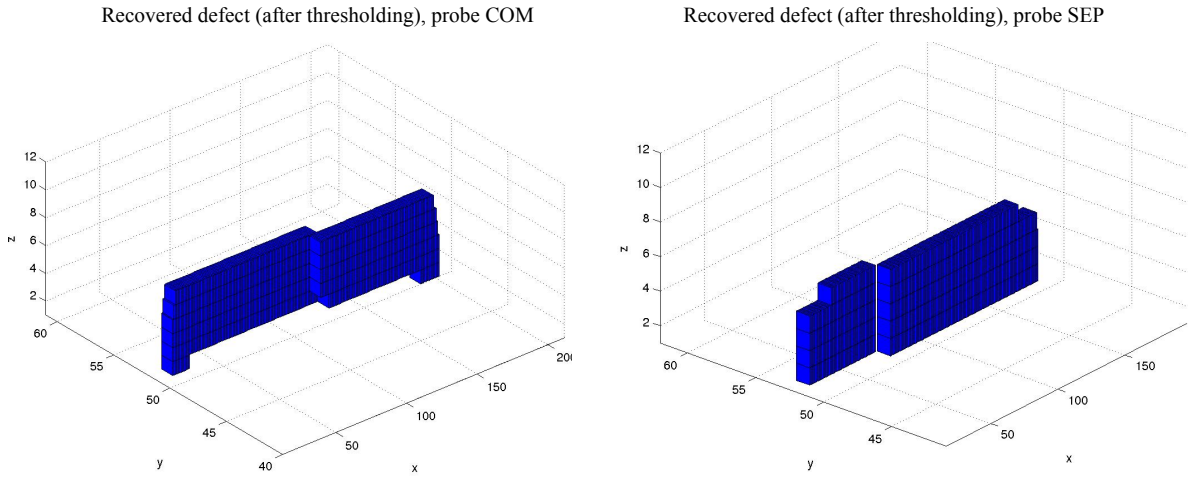

Figure 7 3D reconstruction results on a 3 mm depth crack for COM probe (left hand side) and SEP probe (right hand side). The estimated depth are about 3mm for the COM probe, and 2.5 mm for the SEP probe.

4. Conclusion and perspectives

In this paper we presented a method based on the regularization of inverse problems that provides estimates of the characteristics of unknown defects. The results obtained on mock-ups are very satisfying and suggest that the proposed method could be used in the following way: for defects with depth below 5 mm, either it enables us to know if the depth is between 3 and 5 mm, or it can provide a good estimate of the depth (between 0 and 3 mm). For defects deeper than 5 mm, ultrasonic techniques should be used.
Further investigations are in progress in order to improve both methodological and practical aspects. We are currently working on the parameterization of the defects in order to take into account a known shape for a defect to be recovered. Moreover, we plan to improve the vertical discretization (along the depth) of the inspected medium, by taking thinner layers near the surface (corresponding to the main sensitivity areas of the probe), and bigger layers for deeper ones. The practical application of this method to real defects coming from industrial components is also under study.

References

[1] S. Dubost, Y. Goussard, L. Châtellier, R. Guichard, "Regularization approach for inverse problems in order to characterize defects by eddy current NDE", Advances in Signal Processing for non destructive evaluation of material, Proceedings of the Vth International workshop, Quebec , Canada, 2-4th of August 2005

[2] G. Demoment, "Image Reconstruction and Restoration: Overview of Common Estimation Structure and Problems," *IEEE Trans. Acoustics, Speech and Signal Proc.*, vol. ASSP-37, no 12, pp. 2024-2036, 1989.

[3] J. A. Fessler and S. D. Booth, "Conjugate-Gradient Preconditioning Methods for Shift-Variant PET Image Reconstruction," *IEEE Trans. Image Proc.*, vol. 8, no 5, pp. 688-699, 1999.

[4] G. H. Golub, M. Heath and G. Wahba. "Generalized Cross-Validation as a Method for Choosing a Good Ridge Parameter," *Technometrics*, vol. 21, no. 2, pp. 215-223, 1979.

[5] A. H. Delaney and Y. Bresler, "Globally Convergent Edge-Preserving Regularized Reconstruction: An Application to Limited-Angle Tomography," *IEEE Trans. Image Proc.*, vol. 7, no 2, pp. 204-221, 1998